Journal of Applied Electrochemistry **33**: 1085–1092, 2003.

Electrodeposition of Co–Cu alloy coatings from glycinate baths

A.E. MOHAMED[1], S.M. RASHWAN[1,*], S.M. ABDEL-WAHAAB[2] and M.M. KAMEL[1]
[1]*Chemistry Department, Faculty of Science, Suez Canal University, Ismailia, Egypt*
[2]*Chemistry Department, Faculty of Science, Ain Shams University, Cairo, Egypt*
*(*author for correspondence)*

Received 24 July 2002; accepted in revised form 10 June 2003

Key words: Co–Cu alloys, electrodeposition, glycinate baths

Abstract

The cathodic polarization, cathodic current efficiency of codeposition, composition and structure of Co–Cu alloy as a function of bath composition, current density and temperature were studied. Electrodeposition was carried out from solutions containing $CuSO_4 \cdot 5H_2O$, $CoSO_4 \cdot 7H_2O$, Na_2SO_4 and NH_2CH_2COOH. The cathodic current efficiency of codeposition (CCE) was high and it increased with increasing temperature and Cu^{2+} content in the bath, but it decreased with current density. The codeposition of Co–Cu alloys from these baths can be classified as regular. The Co content of the deposit increased with Co^{2+} content and current density and decreased with glycine concentration and temperature. The structure of the deposited alloys was characterized by anodic stripping and X-ray diffraction techniques. The data showed that the deposited alloys consisted of a single solid solution phase with a face-centred cubic (f.c.c.) structure.

1. Introduction

The electrodeposition of Co–Cu alloys is of great interest because they are used in a variety of industrial applications. Co–Cu alloys with high cobalt content can be used for catalytic purposes [1, 2]. Like Ni–Cu alloys, they are characterized by good corrosion resistance [3, 4]. In recent years, Co–Cu alloys have been widely used as nonmagnetic materials and as electrical resistance devices [5].

The electrodeposition of cobalt–copper alloys has received little attention. Fink and Hutton [6] electrolysed a solution of copper and cobalt sulphates. The deposits were nonuniform, consisting of white and reddish areas. Electrodeposits of copper–cobalt alloys containing up to 70.83% Co were obtained by Shuisheng [7]. Kharlamov *et al.* [8] electrodeposited Cu–Co alloy from pyrophosphate solutions. The solutions contained 300 g L^{-1} $K_4P_2O_7$ and 30 g L^{-1} $CoCl_2 \cdot 6H_2O$ with $CuSO_4 \cdot 5H_2O$ ranging from 1 to 20 g L^{-1}. Anton *et al.* [9] electrodeposited Cu–Co films from citrate baths, and studied the influence of plating parameters such as bath composition, working electrode potential and intensity of agitation on the deposit. Gomez *et al.* [10] used another citrate bath to electrodeposit Cu/Co compositionally modulated multilayers under potentiostatic conditions. They used a bath consisting of 0.25 M sodium citrate, 0.7 M $CoSO_4$ and 0.004–0.008 M $CuSO_4$. Citrate medium was used to maintain the solution pH, in order to minimize hydrogen evolution during deposition and also for its leveling action.

Several authors studied the pulse plating of copper–cobalt alloys. They used different electrolytes such as sulfate and sulfamate solutions with and without boric acid. Sophisticated formulations containing surfactants and brighteners were also used [11–14].

The most common baths containing complexing agents, are cyanide-based for the deposition of brass, bronze and ternary alloys. The major disadvantage of such baths is their toxicity. Various other complexing agents have been used such as fluoborates, sulfamates, tartrates, citrates and gluconates. These complexing agents are nontoxic and, upon degradation, the effluents are easier to treat than cyanide.

The aim of the present work is to study the electrodeposition of Co–Cu alloys from alkaline glycinate baths. Such baths are not only cheap but also environmentally friendly. The effect of bath composition and some operating parameters on cathodic polarization and cathodic current efficiency was investigated. The composition and quality of the deposits were also examined.

2. Experimental details

Cobalt–copper alloys were obtained from baths of composition: 0.004–0.08 M $CuSO_4 \cdot 5H_2O$, 0.004–0.106 M $CoSO_4 \cdot 7H_2O$, 0.14 M Na_2SO_4 and 1.06–1.6 M NH_2CH_2COOH. All solutions were freshly prepared with distilled water and analytical grade reagents. The pH was adjusted using sulphuric acid or sodium

hydroxide and was measured using a Fisher Scientific pH meter.

The experimental setup consisted of a rectangular Perspex cell equipped with a plane steel cathode and a platinum sheet anode. The percentage composition of the steel cathode was C 0.08; Si 0.01; Mn 0.30; P 0.025; S 0.025; Al 0.045 (a local product of the Egyptian Iron and Steel Company). Each electrode had dimensions of 2.5 cm × 3 cm. The cathode was mechanically polished with increasingly fine grades of emery paper, washed with distilled water, rinsed with ethanol and weighed. The deposition was carried out from stagnant solutions. Experiments were conducted at the required temperatures with the help of an air thermostat ±1 °C. The plating time was 15 min, after which the cathode was withdrawn, washed with distilled water, dried and weighed. The alloy composition was determined via atomic absorption spectrophotometry (AAS) Perkin–Elmer model 2380, after dissolving the deposited alloy in concentrated hydrochloric acid (32%) and diluting the solution with distilled water to 100 mL.

The galvanostatic cathodic polarization measurements were conducted in a three-electrode cell provided with a steel cathode rod of area 0.785 cm^2. A platinum wire was used as an anode and saturated calomel (SCE) as a reference electrode. The potential of the working electrode was measured by a potentiometer (Sargant Welch Scientific Co., USA). The current was applied in 2 mA increments and the corresponding potential was measured.

The anodic stripping voltammetry measurements were made in the three-electrode cell, where the working electrode was a glassy carbon disc of area 0.196 cm^2. The counter electrode was a platinum wire together with a saturated calomel electrode (SCE). These were connected to a potentiostat (model 273) and an X-Y recorder (model RE 0091). The alloys were deposited from selected baths onto glassy carbon electrodes at a particular potential (deposition potential) for a certain time. Each deposition was followed directly by linear potential scan stripping voltammetry with scan rate of 10 mV s^{-1} without removing the electrode from the plating solution.

The phase and crystal structure of the as-deposited binary alloy films were investigated using a Siemens D 500 X-ray diffractometer at 35 kV and 15 mA.

3. Results and discussion

3.1. *Cathodic polarization*

Figure 1 shows the galvanostatic cathodic polarization curves for the deposition of copper (curve a), cobalt (curve b) and Co–Cu alloy (curve c) under identical conditions. The individual discharge of each metal is accompanied by large polarization. On switching from simple to complex electrolytes polarization increases. Copper is predominantly present as $[Cu(NH_2CH_2COO)_2]$ complex, in addition to other complex species. Cobalt mainly exists as $[Co(NH_2CH_2COO)_2]$ complex [15]. At low current densities (below 24 mA cm^{-2}), the polarization curve of Cu lies at considerably more positive potentials than Co. Copper deposition begins, even at 0.04 M, early than cobalt deposition. This result indicates that copper is the nobler metal in the present system. At higher current densities (above 24 mA cm^{-2}), a crossing of copper and cobalt curves was observed, which may be ascribed to a large increase of hydrogen evolution on cobalt.

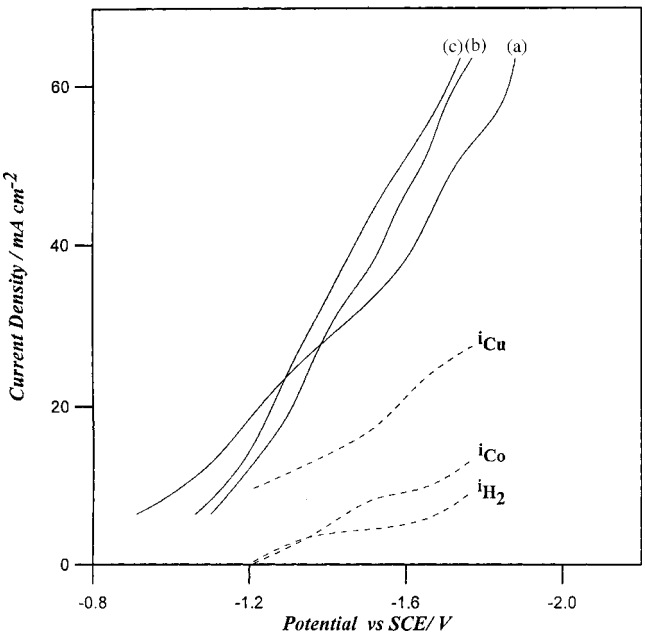

Fig. 1. Galvanostatic cathodic polarization curves (- - - -) obtained at pH 10 and 25 °C for the electrodeposition of (a) copper from solution containing 0.04 M $CuSO_4 \cdot 5H_2O$; (b) cobalt from solution containing 0.106 M $CoSO_4 \cdot 7H_2O$; (c) Co–Cu alloy from solution containing 0.04 M $CuSO_4 \cdot 5H_2O$ and 0.106 M $CoSO_4 \cdot 7H_2O$. Each solution contained 0.14 M Na_2SO_4 and 1.06 M NH_2CH_2COOH. (···) Calculated curves for Cu, Co and H_2.

At low current densities the alloy polarization curve lies at the right of the curves for the pure metals. Either a significant free energy change or some kinetic factor may cause the position of the alloy deposition curve at less noble potentials. However, at high current densities, the alloy polarization curve lies between those of the parent metals. The codeposition enables the less noble metal (Co) to deposit at more positive potentials and causes the more noble metal (Cu) to deposit at more cathodic potentials than in the individual deposition case [16].

The partial polarization curves of each metal and hydrogen during codeposition was computed with the aid of the experimentally determined alloy composition over the range of current density used [16]. The computed partial polarization curves of Cu, Co and H_2 are plotted in Figure 1, (the dotted curves). The partial cathodic polarization curves for the metals differ greatly from the corresponding polarization curves for the individual deposition. The codeposition has shifted

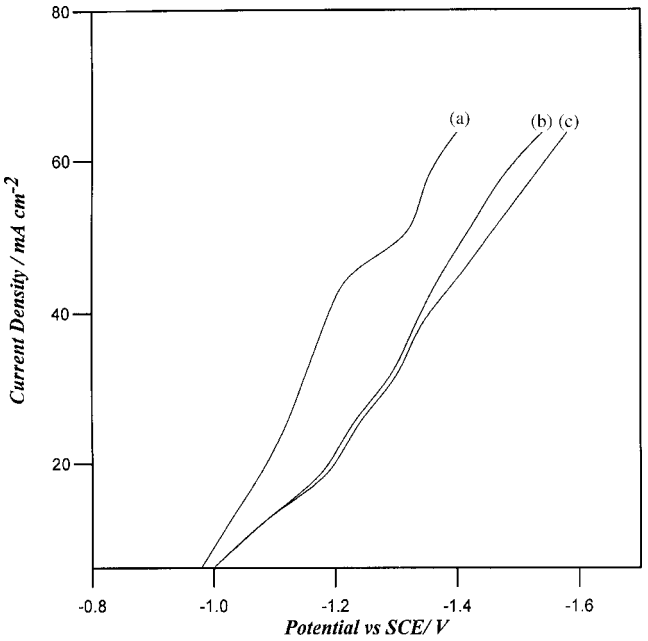

Fig. 2. Galvanostatic cathodic polarization curves for the deposition of Co–Cu alloy on steel at pH 10 and 25 °C from solutions containing 0.04 M $CuSO_4 \cdot 5H_2O$, 0.106 M $CoSO_4 \cdot 7H_2O$ and 0.14 M Na_2SO_4 and different concentrations of NH_2CH_2COOH: (a) 1.06, (b) 1.33 and (c) 1.6 M.

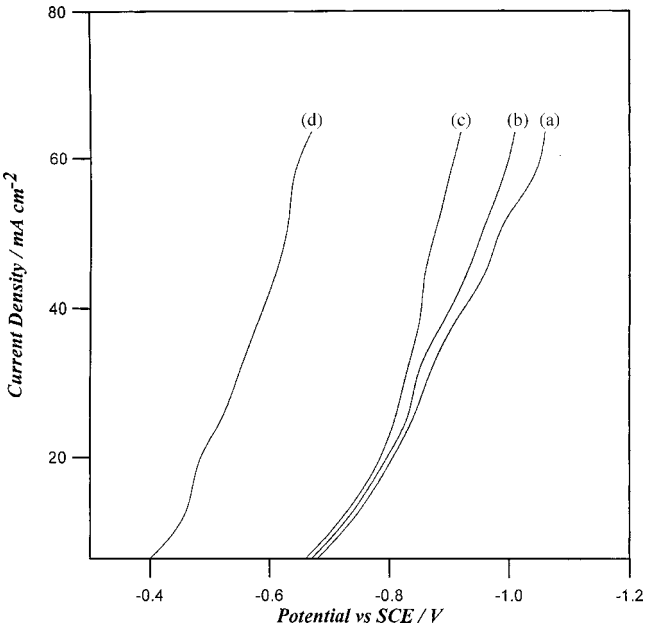

Fig. 3. Galvanostatic cathodic polarization curves for the deposition of Co–Cu alloy on steel at pH 10 and 25 °C from solutions containing 0.04 M $CuSO_4 \cdot 7H_2O$, 0.106 M $CoSO_4 \cdot 7H_2O$, 0.14 M Na_2SO_4 and 1.06 M NH_2CH_2COOH at pH 10 and at different temperatures: (a) 25, (b) 35, (c) 45 and (d) 55 °C.

the deposition potential of Co to more negative values than that of copper. It is obvious that the partial current density of Cu is higher than that of Co and, therefore, Cu deposition proceeds preferentially at the expense of Co deposition. The rate of Co deposition is lower than that of Cu but higher than the rate of hydrogen evolution, Figure 1.

Figure 2 shows that the cathodic polarization of alloy deposition increases with increasing glycine concentration. This is mainly attributable to the increased stability of Cu and Co–glycinate complexes. Increasing the bath temperature decreases the cathodic polarization, Figure 3. This is due to a decrease in the activation polarization of the reduction processes. On the other hand, increasing temperature increases the rate of diffusion of depositable species in the cathode diffusion layer. This decreases the concentration polarization.

3.2. *Composition of Co–Cu electrodeposited alloy*

The cathodic current efficiency and composition of the binary Co–Cu alloy as a function of some plating variables was plotted in Figures 4 to 8. Generally, the cathodic current efficiency, CCE, for the deposition of Co–Cu alloys was high but did not approach 100% due to simultaneous discharge of hydrogen ions. The composition curves of the less noble metal, Co, lie below the composition references line (CRL) (the reference line CRL represents the percentage Co in the bath). These results indicate that Cu is preferentially deposited at the expense of Co. This behaviour is characteristic of plating from regular systems [16].

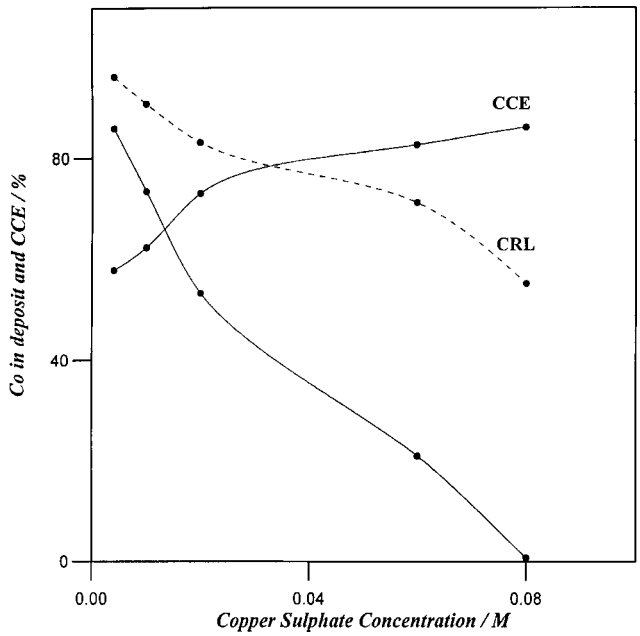

Fig. 4. Effect of $CuSO_4 \cdot 5H_2O$ concentration on CCE and percentage of Co in the deposits from bath containing 0.106 M $CoSO_4 \cdot 7H_2O$, 0.14 M Na_2SO_4 and 1.06 M NH_2CH_2COOH at c.d. = 4.32 mA cm^{-2}, pH 10, t = 15 min and 25 °C. CRL represents the percentage of Co in the bath.

Figure 4 shows the effect of $CuSO_4 \cdot 5H_2O$ concentration on the percentage of cobalt in the deposit and on the CCE of the alloy deposition. The cobalt percentage in the deposit markedly decreases with copper content in the bath due to a significant increase in the efficiency of Cu deposition. As the concentration of $CuSO_4 \cdot 5H_2O$

reaches 20 g dm^{-3}, cobalt deposition ceases entirely and the deposit consists only of copper. Increasing the bath Cu^{2+} content improves the CCE of codeposition. An increase in Cu^{2+} concentration tends to oppose the depletion of copper ions in the cathodic diffusion layer [17].

Figure 5 illustrates the relation between the percentage of cobalt in the deposit and its concentration in the bath. The cobalt percentage in the deposit increases with increasing bath cobalt content. An increase in cobalt concentration tends to ameliorate the depletion of cobalt ions in the cathodic diffusion layer. As shown in Figure 5, increasing Co^{2+} concentration causes a slight increase in the CCE of codeposition.

Inspection of Figure 6 reveals that an increase in the glycine concentration causes a decrease in the percentage of cobalt in the deposit. This is mainly attributable to an increase in the stability of Co^{2+}–glycinate complex species and consequent inhibition of the reduction of cobalt at the expense of the reduction of copper and hydrogen. Increasing the glycine concentration has no effect on the cathodic current efficiency of alloy deposition.

Figure 7 shows the effect of current density on the alloy composition and on the current efficiency for alloy deposition. As the current density increases, the CCE of codeposition decreases as a result of increasing the cathodic polarization, which assists hydrogen evolution. The cobalt content in the deposit increases with current density. Since Cu is deposited preferentially, the cathode film is relatively more depleted in Cu^{2+} ions than in Co^{2+} ions. Therefore, the Cu percentage of the deposit

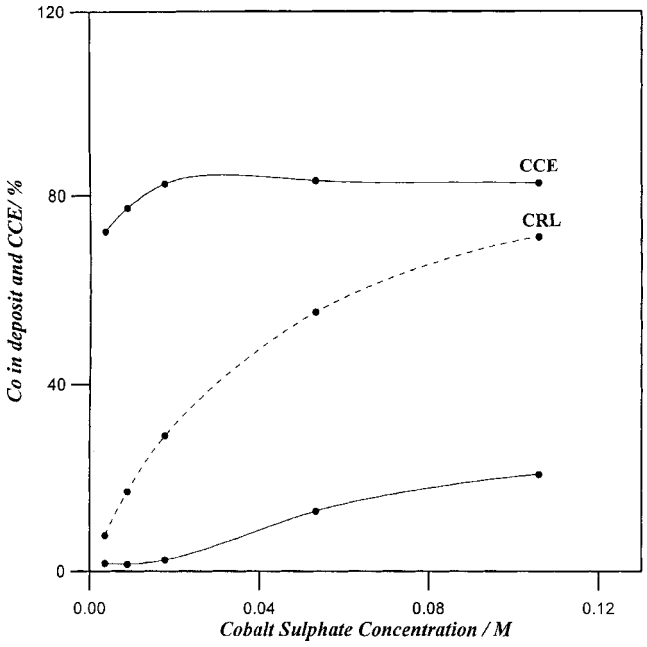

Fig. 5. Effect of $CoSO_4 \cdot 7H_2O$ concentration on CCE and percentage of Co in the deposits from bath containing 0.04 M $CuSO_4 \cdot 5H_2O$, 0.14 M Na_2SO_4 and 1.06 M NH_2CH_2COOH at c.d. = 4.32 mA cm^{-2}, pH 10, t = 15 min and 25 °C. CRL represents the percentage of Co in the bath.

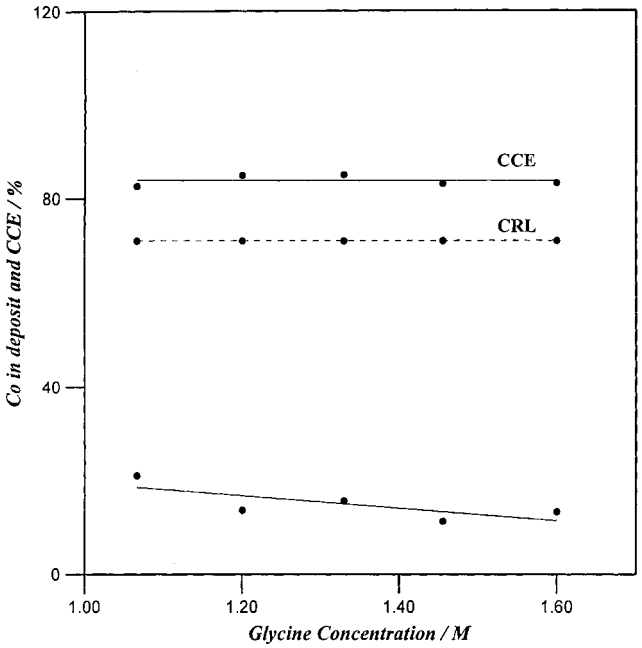

Fig. 6. Effect of NH_2CH_2COOH concentration on CCE and percentage of Co in the deposits from bath containing 0.04 M $CuSO_4 \cdot 5H_2O$, 0.106 M $CoSO_4 \cdot 7H_2O$ and 0.14 M Na_2SO_4 at c.d. = 4.32 mA cm^{-2}, pH 10, t = 15 min and 25 °C. CRL represents the percentage of Co in the bath.

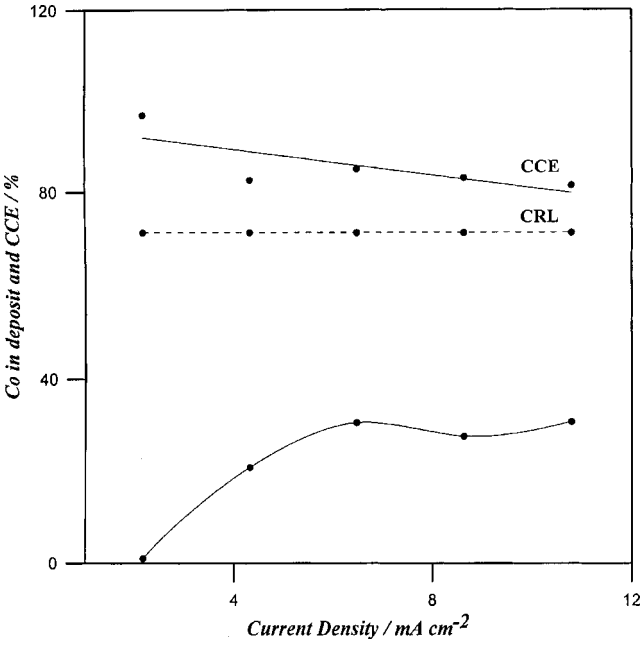

Fig. 7. Effect of current density on CCE and percentage of Co in the deposits from bath containing 0.04 M $CuSO_4 \cdot 5H_2O$, 0.106 M $CoSO_4 \cdot 7H_2O$, 0.14 M Na_2SO_4 and 1.06 M NH_2CH_2COOH at pH 10, t = 15 min and 25 °C. CRL represents the percentage of Co in the bath.

decreases while Co percentage tends to increase with current density. As already noted in regular codeposition, the content of the less noble metal in the deposit increases with current density [16].

Increasing the bath temperature from 10 to 55 °C markedly decreases the cobalt content in the deposit and

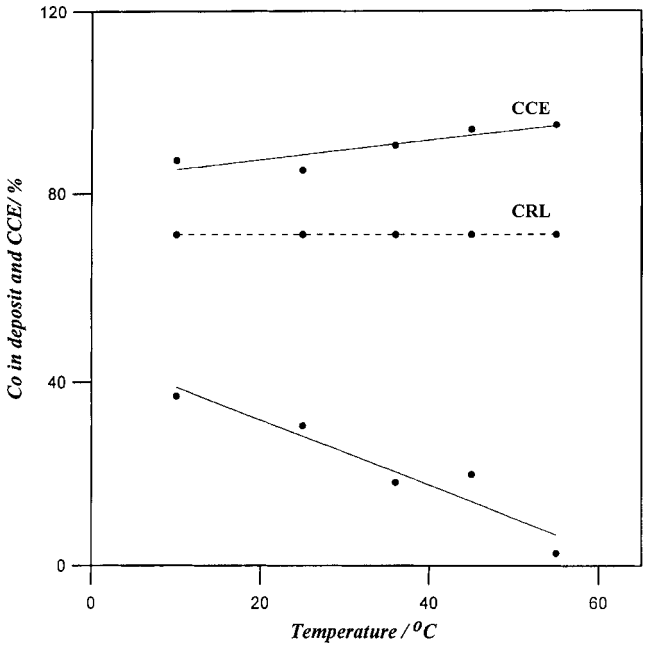

Fig. 8. Effect of temperature on CCE and percentage of Co in the deposits from bath containing 0.04 M $CuSO_4 \cdot 5H_2O$, 0.106 M $CoSO_4 \cdot 7H_2O$, 0.14 M Na_2SO_4 and 1.06 M NH_2CH_2COOH at c.d. = 6.48 mA cm^{-2}, pH 10 and $t = 15$ min. CRL represents the percentage of Co in the bath.

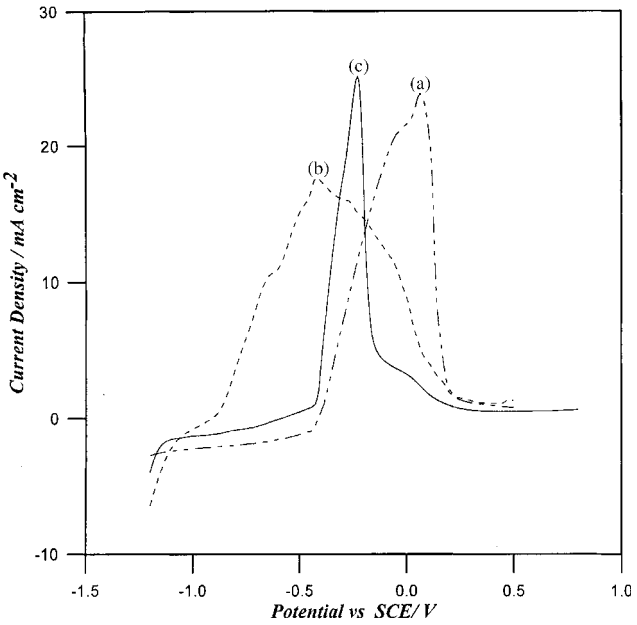

Fig. 9. Linear sweep voltammogram of a fixed glassy carbon electrode in various solutions: (a) 0.04 M $CuSO_4 \cdot 5H_2O$ (deposition potential −1.2 V vs SCE) (b) 0.106 M $CoSO_4 \cdot 7H_2O$ (deposition potential −1.3 V vs SCE) (c) 0.04 M $CuSO_4 \cdot H_2O$ and 0.106 M $CoSO_4 \cdot 7H_2O$ (deposition potential = −1.1 V vs SCE). Each solution containing 0.14 M Na_2SO_4 and 1.06 M NH_2CH_2COOH. Sweep rate 10 mV s^{-1}.

increases the current efficiency for alloy deposition, Figure 8. Increasing the temperature enhances the concentration of metal ions in the cathode diffusion layer because the rates of diffusion and convection increase with temperature. Under these conditions, copper is deposited at the expense of cobalt.

3.3. *Anodic linear stripping voltammetry*

To analyse the alloy deposits in situ, potentiodynamic anodic stripping was carried out since this method has been shown to be useful in the characterization of deposited alloy [18]. Figure 9 illustrates the stripping voltammograms of pure copper (curve a), pure cobalt (curve b) and Co–Cu alloy (curve c) deposited under the same conditions. The voltammograms of the alloy and the pure metals have only one dissolution peak. The dissolution peak of pure Cu appears at a more positive potential than that of pure Co. The alloy dissolution peak appears at intermediate potential between the potentials of the dissolution peaks of pure cobalt and pure copper. This indicates that the structure of the

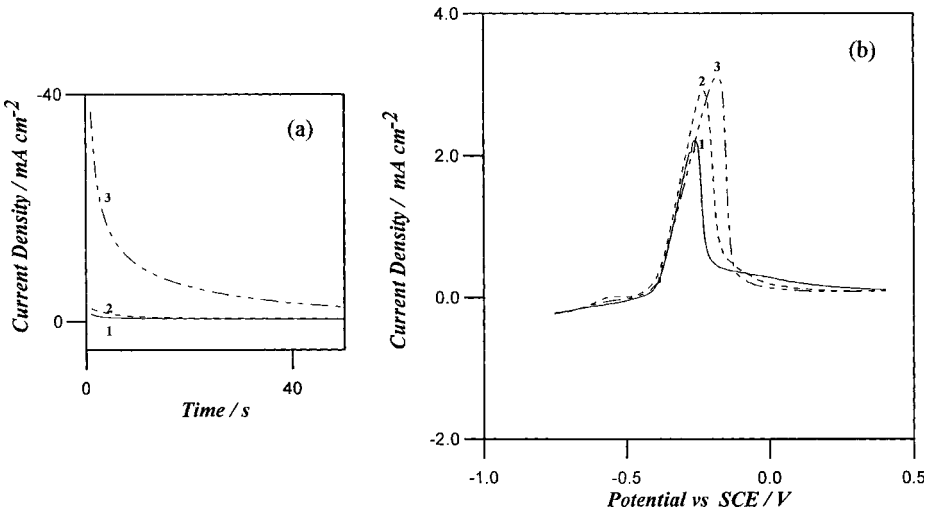

Fig. 10. Potentiostatic j/t transients of deposition (a) and corresponding linear sweep voltammograms of dissolution (b) of Co–Cu alloy, obtained from solution containing 0.04 M $CoSO_4 \cdot 5H_2O$, 0.106 M $CoSO_4 \cdot 7H_2O$, 0.14 M Na_2SO_4 and 1.06 M NH_2CH_2COOH. Applied deposition potentials: (a) −0.3, (b) −0.7 and (c) −1.1 V. Sweep rate 10 mV s^{-1}.

deposit is similar to that of the pure metals [19]. The appearance of a single peak indicates that the alloy consists of one phase (solid solution). The two components (Co and Cu) dissolve simultaneously so that the resulting voltammogram shows only one peak.

Swathirajan [18] reported that the LSV of dissolution of solid solution should have two separate peaks. The first corresponds to preferential dissolution of the less noble component at more negative potentials. However, the experimentally recorded LSVs of dissolution of electrodeposited thin layers of cobalt–copper alloys, contradict this theory. The dissolution of the cobalt–copper alloys takes place through one peak only. The same result was reported by Abd El-Rehim *et al.* [20].

Figure 10 displays the potentiostatic j/t transients of deposition of thin layers of Co–Cu alloy on glassy carbon. It also shows the corresponding LSVs of dissolution of these alloys in the same solution. At all examined potentials, the LSV has only one dissolution peak which arises from the simultaneous dissolution of both Co and Cu from their solid solutions. Increasing the deposition potential shifts the peak potential into the noble direction and increases the peak size, Figure 10(b). This is mainly attributed to an increase in the deposit amount with the applied potential.

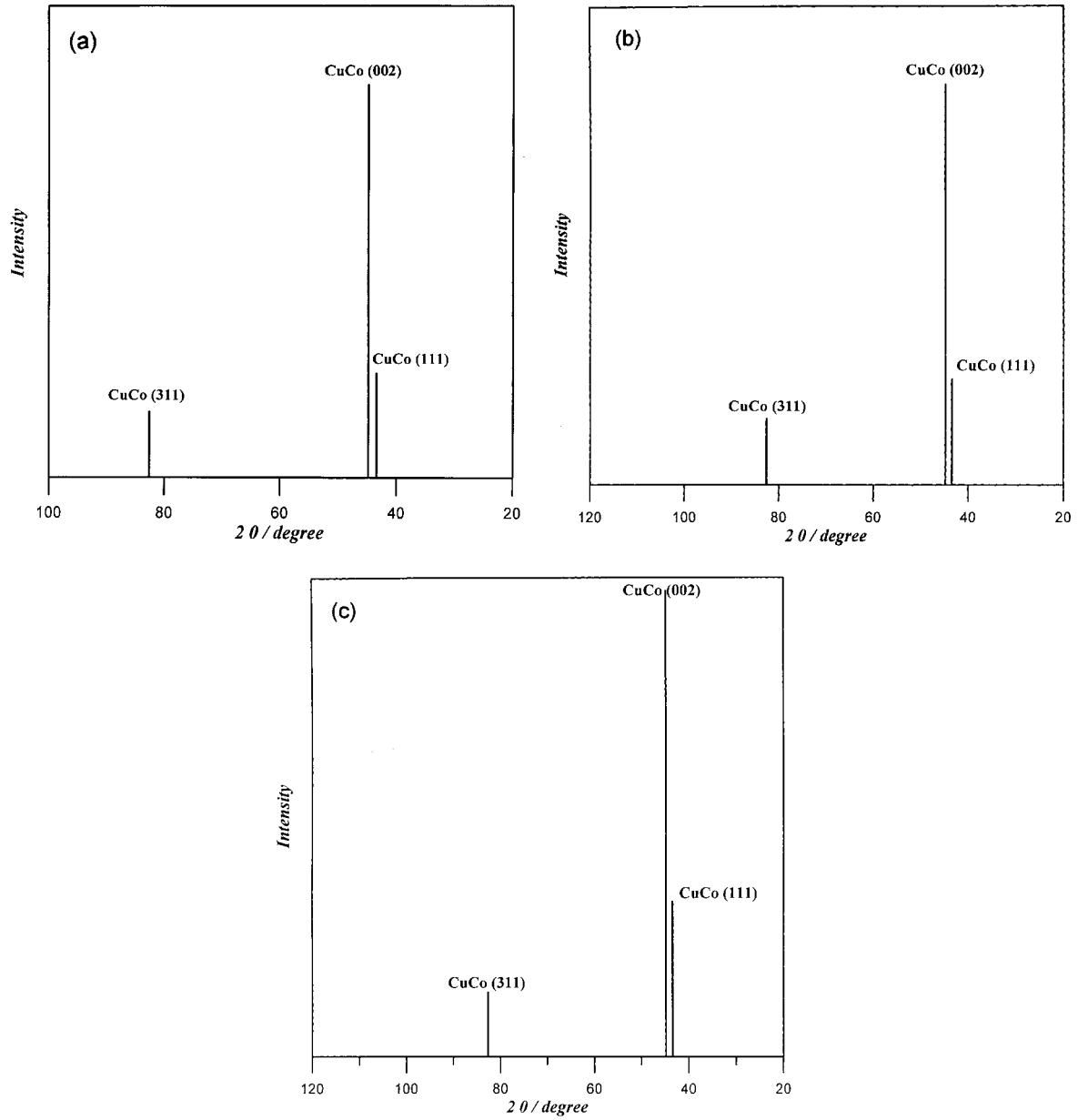

Fig. 11. X-ray diffraction patterns of electrodeposited Co–Cu alloy obtained from a bath containing 0.04 M $CuSO_4 \cdot 5H_2O$, 0.106 M $CoSO_4 \cdot 7H_2O$, 0.14 M Na_2SO_4 and 1.06 M NH_2CH_2COOH at pH 10, $t = 15$ min, 25 °C and at different current densities: (a) 4.32, (b) 6.48 and (c) 10.80 mA cm^{-2}.

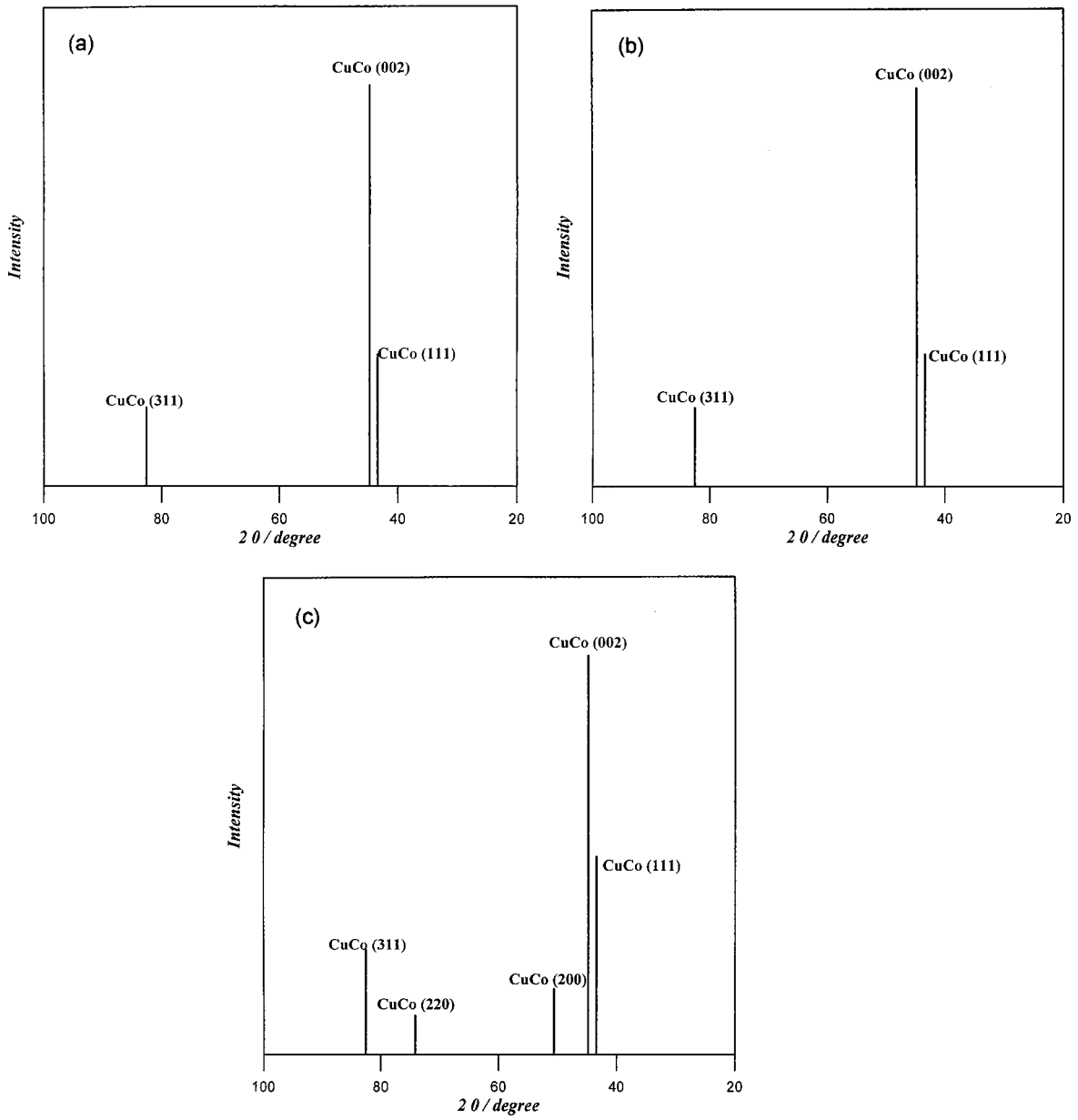

Fig. 12. X-ray diffraction patterns of electrodeposited Co–Cu alloy obtained from a bath containing 0.04 M $CuSO_4 \cdot 5H_2O$, 0.106 M $CoSO_4 \cdot 7H_2O$, 0.14 M Na_2SO_4 and 1.06 M NH_2CH_2COOH at c.d. = 6.48 mA cm^{-2}, pH 10, t = 15 min. at different temperatures: (a) 10, (b) 25 and (c) 55 °C.

3.4. *Structure of the deposits*

X-ray diffraction measurements were carried out on Co–Cu electrodeposits obtained under different experimental conditions. The diffractograms exhibit only lines corresponding to the face-centred cubic (f.c.c.) structure with lattice parameter values ranging from 360.8 to 404.2 pm (picometre) [21]. The peaks are sharp and well defined, indicating good crystallization. The diffractograms indicate that the alloy deposits have a preferred orientation of (002). The observation of a single diffraction angle for the planes (002) can be interpreted such that copper and cobalt share the same lattice parameter and that interfaces between copper and cobalt are coherent [22].

The effect of current density on XRD patterns of electrodeposited Co–Cu alloy is shown in Figure 11. The (002) plane is the major one and appears in all the examined deposits but with different intensities. Increasing the current density leads to an increase in the intensity of plane (111). A new diffraction plane, (200), appears with low intensity. Increasing the bath temperature improves the intensity of the planes (002) and (111). At 55 °C, two new diffraction planes, (200) and (220), appear but with low intensity, Figure 12.

4. Conclusions

Smooth, compact and bright Co–Cu binary alloys were electroplated satisfactorily on steel sheet from baths

containing cobalt sulfate, copper sulfate, sodium sulfate and glycine (pH 10 ± 0.2). The effects of bath composition, current density and temperature on cathodic polarization, cathodic current efficiency of codeposition, and deposited alloy structure were investigated. The cathodic current efficiency of the bath was relatively high and increased with increasing temperature and bath metal content. The composition of the deposits is strongly dependent on bath temperature and current density. The deposited alloys consisted of a single solid solution phase with a face-centred cubic structure.

References

1. E. Endoh, T. Otouma and Y. Oda, *J. Hydrogen Energy* **12** (1987) 473.
2. Ph. Vermeiren, R. Leysen and H. Vandenborre, *Electrochim. Acta* **30** (1985) 1253.
3. J. Crousier and I. Bimajhra, *J. Appl. Electrochem.* **23** (1993) 780.
4. J. Horkans, I.C.H Chang, P.C. Andricacos and E.J. Podlaha, *J. Electrochem. Soc.* **138** (1991) 411.
5. L. Brossard and B.I. Marquis, *J. Hydrogen Energy* **19** (1994) 231.
6. C.G. Fink and J.L. Hutton, *Trans. Electrochem. Soc.* **85** (1944) 119.
7. W. Shuisheng, MSc thesis, Laurentian University of Sudbury, Canada (1989).
8. V.I. Kharlamov, O.M. Belous, N.S. Grigoryan, V.V. Terekhova and T.A. Vagramyan, *Russ. J. Electrochem.* **33**(1) (1997) 84.
9. R.L. Anton, M.L. Fdez-Gubieda, A.G. Arribas, J. Herreros and M. Insausti, *Mater. Sci. Eng.* **A 335** (2002) 94.
10. E. Gomez, A. Labarta, A. Llorente and E. Valles, *Surf. Coat. Technol.* **153** (2002) 251.
11. M. Alper, W. Schwarzacher and S.J. Lane, *J. Electrochem. Soc.* **144** (1997) 2346.
12. Y. Jyoko, S. Kashiwabara and Y. Hayashi, *J. Electrochem. Soc.* **144** (1997) L 193 and 2346.
13. J. Xue, J. Wu and D. Yang, *Acta Metall. Sin.* (*China*) **10**(2) (1997) 115.
14. N. Myung, K.H. Ryu, P.T.A. Sumodojo and K. Nobe, *Proc. Electrochem. Soc.* **97**(27) (1998) 270.
15. P.R. Reddy and V.B. Rao, *Polyhedron* **4**(9) (1985) 1603.
16. A. Brenner, 'Electrodeposition of Alloys', Vol. 1 (Academic, New York, 1963).
17. S.S. Abd El-Rehim, N.F. Mohamed, N.H. Amin and L.I. Ali, *J. Appl. Electrochem.* **27** (1997) 1385.
18. S. Swathirajan, *J. Electrochem. Soc.* **133** (1986) 671.
19. E. Gomez, J. Ramirez and E. Valles, *J. Appl. Electrochem.* **28** (1998) 71.
20. S.S. Abd El-Rehim, S.M. Abd El-Wahaab, S.M. Rashwan and Z.M. Anwar, *J. Chem. Technol. Biotechnol.* **75** (2000) 237.
21. V.M. Lopez-Hirata and E.M. Estrada, *Electrochim. Acta* **42** (1997) 61.
22. P.E. Bradely and D. Landolt, *Electrochim. Acta* **45** (1999) 1077.